

# Dry Sliding Wear Response of Some Bearing Alloys as Influenced by the Nature of Microconstituents and Sliding Conditions

B.K. PRASAD

An attempt has been made in this study to examine the dry sliding wear response of a leaded-tin bronze, an aluminum bronze, and a conventional zinc-based alloy under varying applied pressure and speed conditions. Different characteristics of the microconstituents of the alloys have been correlated with that of their wear behavior. The study clearly indicates that the influence of the microstructural features greatly changes with the sliding conditions. It also has been observed that in order to attain good wear characteristics, a material should comprise an optimum level of lubricating, load bearing and ductile microconstituents, and, above all, thermal stability. Room temperature properties in fact play rather a secondary role in this context.

## I. INTRODUCTION

THERE exist a number of alloys which can be used for a variety of tribological and other engineering applications.<sup>[1-7]</sup> Sliding of one component over/against the other occurs in many situations, bush bearings being one of the important ones.<sup>[1-7]</sup> In general, leaded-tin bronzes are widely used in bush-bearing applications<sup>[1,3,4-6]</sup> while aluminum bronzes are also used under specific service conditions.<sup>[5]</sup> Zinc-based alloys have been found to be cost- and energy-effective substitutes to the bronzes in various sliding wear applications.<sup>[1-3,6,7]</sup> From microstructural considerations, the conventional bronze alloys are quite different from one another. For example, the leaded-tin bronzes contain a considerable quantity of the lubricating phase, lead; the element increases the crack sensitivity of the alloy under specific conditions of sliding.<sup>[8,9]</sup> The aluminum bronzes do not contain any lubricating microconstituent but possess very good thermal stability. Finally, in the case of zinc-based alloys, the major microconstituent (*i.e.*, zinc) is lubricating in nature,<sup>[10]</sup> but the alloys suffer from poor elevated-temperature properties.<sup>[2]</sup>

It may be mentioned that the sliding wear response of materials depends very much on their microstructural features in terms of lubricating properties, crack sensitivity, and thermal stability. In fact, the predominance of the factors under a specific sliding condition essentially controls the wear behavior of the materials. Thus, sliding conditions are the ones to govern the wear response of the materials.

Available information indicates that although the sliding wear behavior of the leaded-tin and aluminum bronzes and zinc-based alloys has been studied to some extent,<sup>[8-22]</sup> yet the role of their microstructural characteristics on the sliding wear response of the alloys has been investigated to a limited extent<sup>[8,9,11,12,15-20]</sup> in spite of their great significance.

In view of this information, an attempt has been made in this study to examine the influence of the role of various microconstituents of a leaded-tin bronze, an aluminum

bronze, and a zinc-based alloy on their sliding wear response under varying conditions of applied pressure and speed. Mechanical properties of the alloys have also been correlated with their wear properties.

## II. EXPERIMENTAL

### A. Alloy Preparation

Alloys (Table I) were prepared by solidifying in the form of 20-mm-diameter, 150-mm-long cylindrical castings using permanent molds. Elements used for preparing the alloys had purity levels above 99.95 pct.

### B. Microstructural Characterization

Microstructural studies of the alloys were carried out using a Leitz (Wetzlar, Germany) optical microscope. The specimens (20-mm diameter, 15-mm height) were metallographically polished and etched. Bronzes were etched with potassium dichromate solution, while dilute aqua regia was used for etching the zinc-based alloy.

### C. Measurement of Mechanical Properties

Hardness of specimens was measured using a Vickers hardness tester at an applied load of 15 kg. An Instron universal testing machine was used for determining the tensile and compressive properties of the alloys. Tensile properties were measured on specimens having 4.0-mm gage diameter, 22-mm gage length, at the strain rate of  $1.52 \times 10^{-3}$ /s. Test temperatures adopted in this case were 35 °C, 60 °C, 100 °C, 150 °C, and 200 °C. Compressive behavior of the 8.0-mm diameter, 15-mm long specimens was studied at 35 °C at the strain rate of  $2.28 \times 10^{-3}$ /s.

Reported values in each case represent an average of three observations.

### D. Sliding Wear Tests

Dry sliding wear tests were conducted on 8.0-mm-diameter, 53-mm-long cylindrical specimens using an EN 25 (Fe-0.3C-0.7Cr-2.5Ni-0.5Mo) steel counterface disc of

---

B.K. PRASAD, Scientist, is with the Regional Research Laboratory, Habibganj Naka, Bhopal 462 026, India.  
Manuscript submitted July 1, 1996.

**Table I. Chemical Composition of the Experimental Alloys**

Serial Number	Alloy	Element (Wt Pct)						
		Zn	Cu	Sn	Pb	Al	Fe	Mg
1	lead-tin bronze	2.90	*	7.20	7.30	—	—	—
2	aluminum bronze	—	*	—	—	9.90	1.20	—
3	zinc-based alloy	*	2.50	—	—	27.50	—	0.03

\*Remainder

hardness RC 32. The test apparatus was a Cameron–Plint (Wokingham, United Kingdom) pin-on-disc machine.<sup>[8,12]</sup> Applied pressures in this study were varied in steps until seizure of the specimens was indicated by abnormal noise and vibration in the pin-disc assembly. Sliding speeds adopted were 0.42 and 4.60 m/s. All the tests were carried out up to a predetermined sliding distance of 500 m except in the event of specimen seizure. In the latter case, tests were stopped as soon as specimens tended to seize. In the case of the lead-tin bronze, the specimens lost proper contact with the disc due to material chipping off at 0.42 m/s even before traversing the specified sliding distance. Tests were stopped as soon as this observation was made.

Wear rates were computed by a weight-loss technique. The specimens were thoroughly cleaned and weighed prior to and after the wear tests. Temperature rise near the mating surface of the specimens was monitored as a function of test duration with the help of a chromel-alumel thermocouple inserted in a hole made at a distance of 1.5 mm from the mating surface.

### III. RESULTS

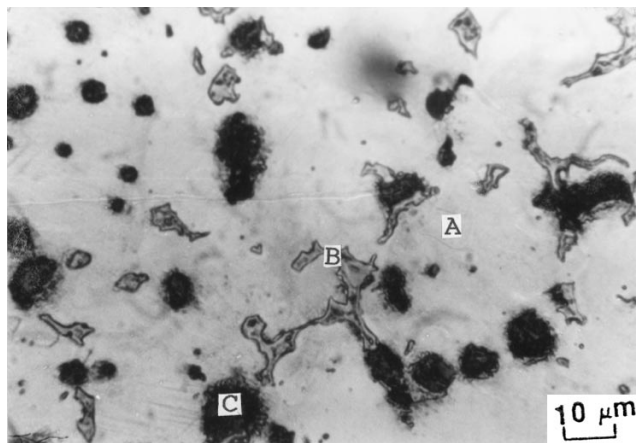
#### A. Microstructure

Figure 1 shows the microstructural characteristics of the alloys. The lead-tin bronze revealed primary  $\alpha$ , Cu-Sn intermetallic compound(s), and particles of lead (Figure 1(a), regions marked by A, B, and C, respectively). Various microconstituents of the aluminum bronze were observed to be primary  $\alpha$ , Cu-Al precipitates, and fine particles of iron (Figure 1(b), regions marked by A, D, and arrow, respectively). Phases present in the zinc-based alloy were primary  $\alpha$ , eutectoid  $\alpha + \eta$ , and the metastable  $\epsilon$  phase (Figure 1(c), regions marked by A, E, and double arrow, respectively).

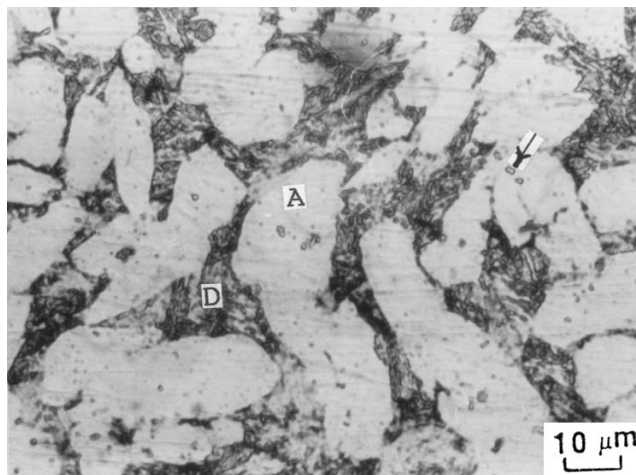
#### B. Mechanical Properties

Table II represents the hardness of the alloys. The aluminum bronze exhibited maximum hardness, while that of the lead-tin bronze exhibited the least, the zinc-based alloy attaining an intermediate hardness value.

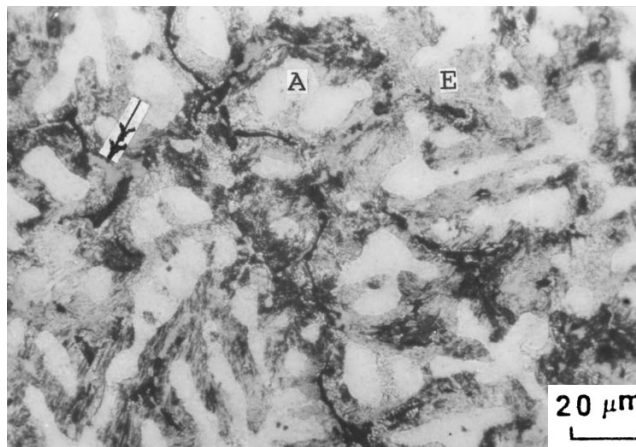
A schematic representation of the response in terms of the reduction in the height of the alloy specimens during the compressive tests is shown in Figure 2. The aluminum bronze displayed superior ultimate compressive strength to that of the lead-tin bronze prior to fragmentation, while the zinc-based alloy tended to get coined during the tests (Figure 2, Table II). Moreover, the extent of the compressive



(a)



(b)



(c)

Fig. 1—Microstructural features of (a) the lead-tin bronze, (b) aluminum bronze, and (c) zinc-based alloy (A:  $\alpha$ , B: Cu-Sn intermetallic phase, C: lead particles, D: Cu-Al phase, arrow: iron particle, E: eutectoid  $\alpha + \eta$ , and double arrow:  $\epsilon$ ).

sive deformation (*i.e.*, the reduction in the height of the specimens) was the maximum for the zinc-based alloy, followed by those of the lead-tin and aluminum bronzes; the latter ones attained comparable extent of compressive deformation (Table II).

**Table II. Hardness and Ultimate Compressive Strength of the Experimental Alloys**

Solution Number	Alloy	Hardness (HV)	Dimensional Changes during Compression (Pct)		Ultimate Compressive Strength (MPa)
			Increase in Diameter	Decrease in Height	
1	lead-tin bronze	76	28	42	900
2	aluminum bronze	162	27	35	1300
3	zinc-based alloy	130	126	78	*

\*Tests stopped since specimens were coined without fracturing and the operating load limit of the machine was reached.

Tensile properties (strength and elongation) of the aluminum bronze were better than that of the zinc-based alloy and lead-tin bronze over the entire range of test temperatures (Figure 3). Further, the zinc-based alloy attained higher tensile strength (Figure 3(a)) and elongation (Figure 3(b)) than the lead-tin bronze at lower temperatures, while the trend reversed, as far as tensile strength is concerned, at higher test temperatures. Moreover, the extent of deterioration in the strength of the zinc-based alloy with temperature was significantly higher than either of the bronzes. The elongation of the lead-tin bronze was least influenced, while in the remaining cases, it increased with temperature (Figure 3(b)).

### C. Sliding Wear Behavior

Figure 4 reveals the wear rate of the alloys plotted as a function of applied pressure at the sliding speeds of 0.42 and 4.60 m/s. The wear rate was observed to increase with load and speed in the case of the aluminum bronze and the zinc-based alloy, while a reverse trend was followed by the lead-tin bronze as far as the influence of sliding speed on wear rate is concerned. Moreover, at 0.42 m/s, two slopes were exhibited by the wear rate vs pressure curves of the zinc-based alloy and the lead-tin bronze (Figure 4), wherein the slope was initially low up to a specific applied pressure and became higher at larger pressures. On the contrary, the aluminum bronze showed three slopes revealing a lower slope in the intermediate pressure range at the speed. The trend changed at the sliding speed of 4.60 m/s in the sense that one and three slopes were observed by the wear rate vs pressure plots of the zinc-based alloy, the aluminum bronze, and the lead-tin bronze, respectively (Figure 4).

A comparison of the wear response of the specimens at 0.42 m/s indicates the least wear rate for the zinc-based alloy (prior to seizure), followed by those of the aluminum bronze and the lead-tin bronze in an ascending order (Figure 4). Regarding their seizure pressure (*i.e.*, resistance to seizure), the aluminum bronze exhibited maximum seizure resistance, whereas that of the zinc-based alloy was slightly less at the speed of 0.42 m/s. No seizure pressure for the lead-tin bronze could be observed in this case since the test was stopped as soon as the specimens lost proper contact with the disc due to material chipping off.

F: Fragmentation  
 x: Operating load limit of the equipment reached  
 ---: Lead-tin and aluminum bronzes  
 —: Zinc-based alloy

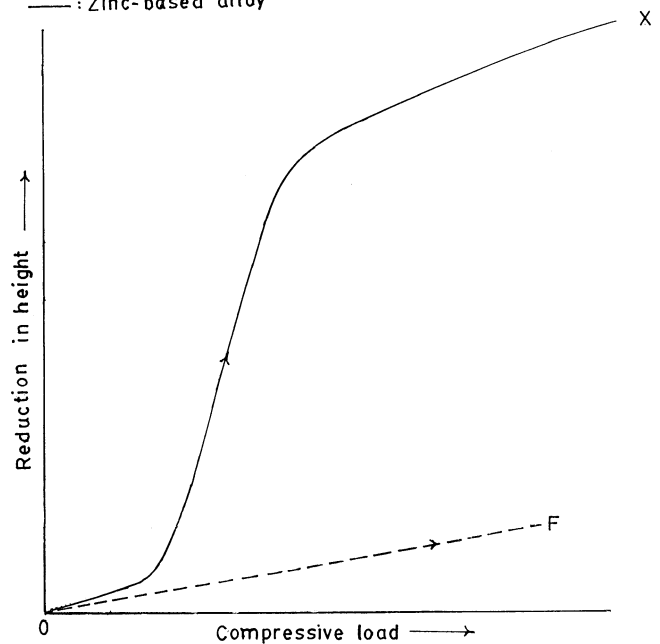


Fig. 2—A schematic representation of the behavior of the alloys under compressive loading.

On the contrary, however, at the sliding speed of 4.60 m/s, the lead-tin bronze delineated the least wear rates, while the zinc-based alloy showed the maximum, and the aluminum bronze experienced intermediate wear rates (Figure 4). The seizure resistance of the lead-tin bronze was maximum. This was followed by that of the aluminum bronze and the zinc-based alloy (Figure 4).

The temperature rise near the mating surface of the specimens plotted as a function of test duration at different pressures and speeds is shown in Figure 5. The rate of temperature rise was significantly higher initially than that at longer test durations. Moreover, a sudden decrease in temperature was observed in the case of the lead-tin bronze at longer test durations at 5.0 MPa when the sliding speed was 0.42 m/s (Figure 5(a)). The zinc-based alloy and the aluminum bronze attained a comparable extent of frictional heating, while that for the lead-tin bronze was the maximum at the lowest pressure (Figure 5(a)). However, the zinc-based alloy showed the least degree of heating followed by that of the aluminum bronze and the lead-tin bronze (in an ascending order) in the intermediate pressure range (5.0 MPa). At high pressures (13.0 MPa), however, the zinc-based alloys suffered from a higher extent of heating than the aluminum bronze (Figure 5(a)). The trend observed by the alloys at 4.60 m/s was different (Figure 5(b)) than that of 0.42 m/s of sliding (Figure 5(a)). In the former case, the lead-tin bronze experienced least frictional heating, while that of the aluminum bronze was maximum at the lowest applied pressure, with the zinc-based alloy showing an intermediate behavior (Figure 5(b)). At higher pressures also, the aluminum bronze showed a significantly higher temperature rise than the lead-tin bronze at the speed of 4.60 m/s (Figure 5(b)).

Figure 6 represents the maximum temperature rise near

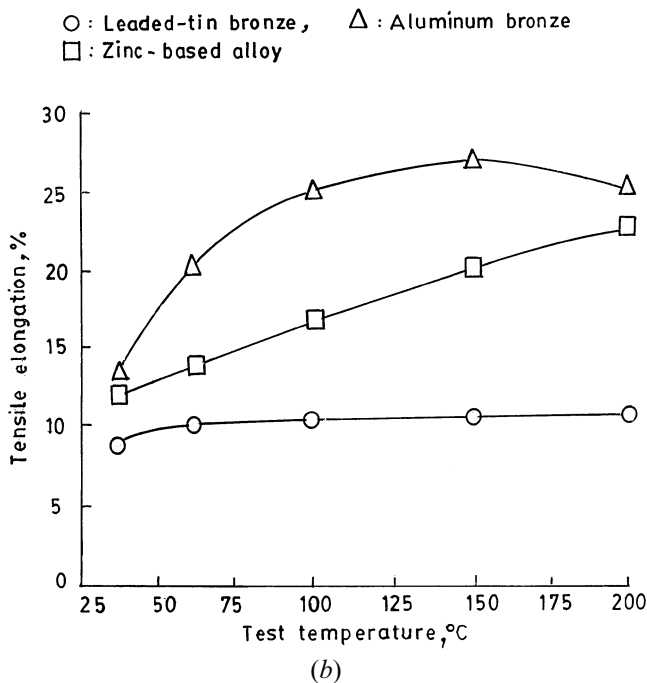
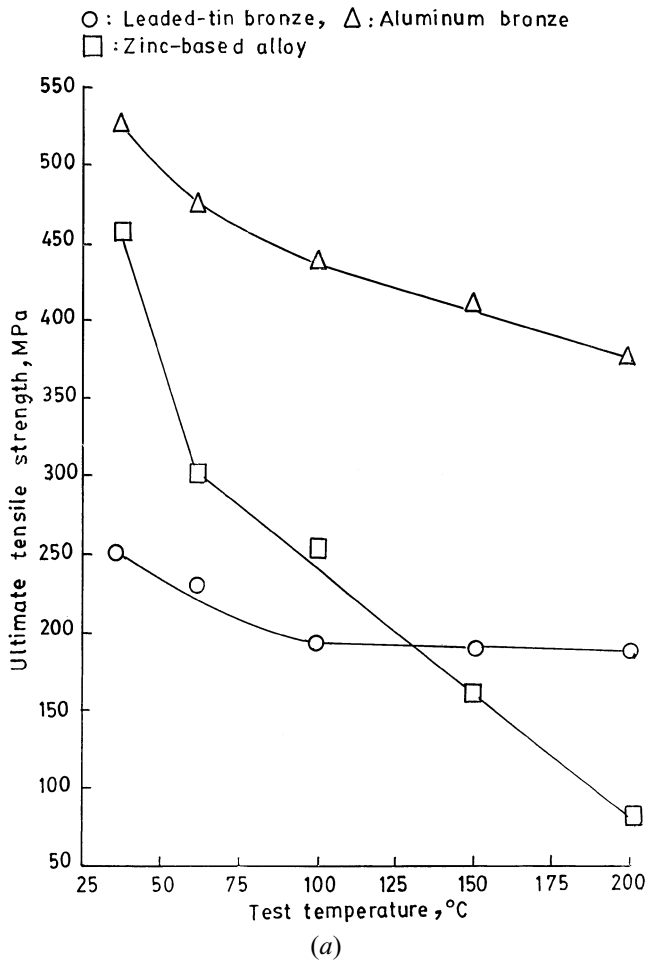


Fig. 3—Tensile properties of the alloys plotted as a function of test temperature: (a) ultimate tensile strength and (b) elongation.

the specimen surface as a function of applied pressure at different speeds of sliding. It may be noted that at 0.42 m/s, the zinc-based alloy experienced the least degree of heating,

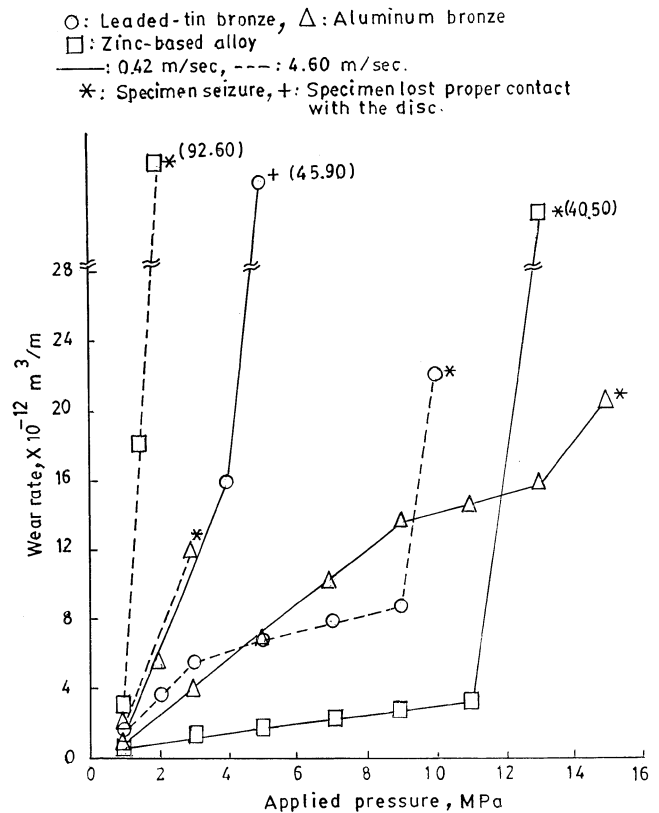


Fig. 4—Wear rate of the alloys plotted as a function of applied pressure at different sliding speeds.

whereas that of aluminum bronze exhibited the maximum, with the lead-tin bronze showing an intermediate response. On the contrary, the lead-tin bronze attained minimum frictional heating, followed by that of the zinc-based alloy and the aluminum bronze when the sliding speed was 4.60 m/s (Figure 6). Further, the zinc-based alloy and the bronze showed the maximum temperature to increase with pressure at a decreased rate at lower pressures, while their seizure tended to increase the rate of heating (Figure 6).

#### IV. DISCUSSION

For a material to perform well in plain bearing applications, it is essential that it contain at least a ductile phase, a load-bearing microconstituent, and a lubricating element/constituent.<sup>[8]</sup> The ductile phase imparts compatibility to the alloy system and provides support to the remaining load-bearing and lubricating microconstituents.<sup>[8]</sup> It has been observed that the microcracking tendency of the alloys plays a negative role, since in such cases, the remaining phases get engulfed in the coarse debris and are removed prematurely without performing their work.<sup>[8]</sup> Thus, the effectiveness with which the microconstituents can play their roles very much depends on the conditions of sliding, and, in fact, the predominance of the effects would decide the wear response of the materials under a given set of working conditions. It may be mentioned that sliding wear involves the generation of a sufficiently high degree of frictional heating because of the adhesion taking place between the mating surfaces during this mode of wear. Adhesion results

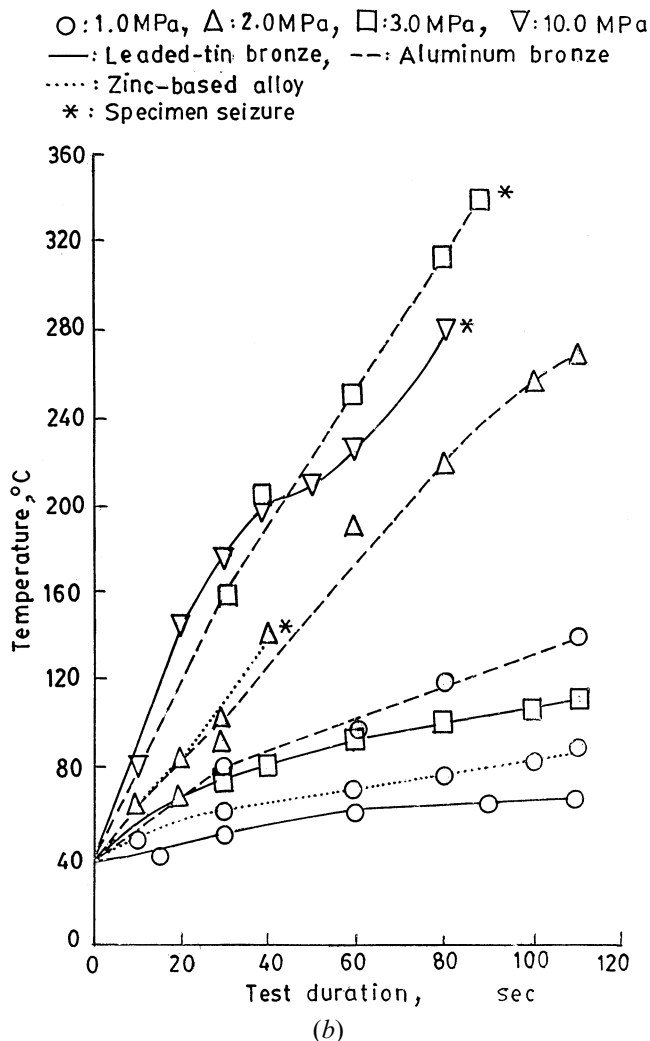
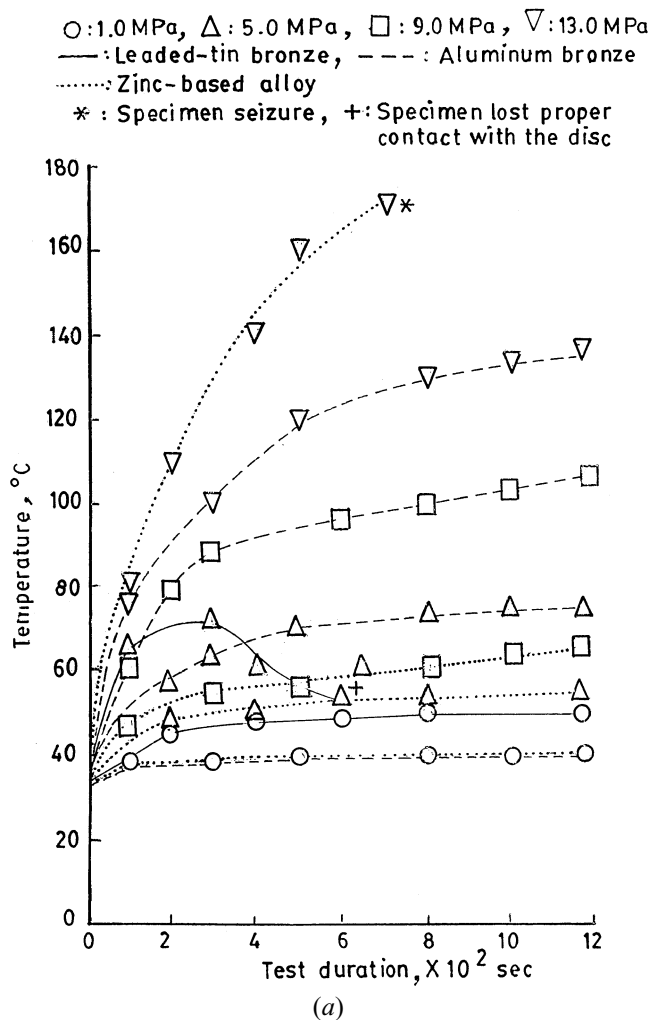


Fig. 5—Temperature rise near the specimen surface as a function of test duration at different pressures at the sliding speed of (a) 0.42 m/s and (b) 4.60 m/s.

from thermal and thermomechanical processes involving severe, localized plastic deformation under the conditions of high rate of straining, leading to the yielding, fragmentation, and entrapment of the contacting asperities in between the mating surfaces during interaction of these surfaces.<sup>[23]</sup> As a result, thermal stability also governs the sliding wear characteristics of the materials to a great extent. In view of these considerations, the wear response of the investigated alloys will now be analyzed.

The leaded-tin bronze consisted of primary  $\alpha$  (copper-rich solid solution of tin), Cu-Sn intermetallic compound, and particles of lead (Figure 1(a), regions marked by A, B, and C, respectively). The  $\alpha$  phase is ductile in nature, which provides compatibility and support to the hard, load-bearing Cu-Sn phase(s) and lubricating lead particles. The degree of the compatibility and support depends greatly on the extent of frictional heating generated during sliding in view of the high melting characteristics of the  $\alpha$  phase.<sup>[8]</sup> Obviously, temperatures above the critical one would improve the mentioned properties of the  $\alpha$  phase; here, the term *critical temperature* is meant to qualitatively indicate a level of temperature at and above which the  $\alpha$  phase attains enough compatibility to accommodate the remaining load-bearing and lubricating microconstituents more effectively. This enables the  $\alpha$  phase to suppress the tendency of the

bronze toward the particle/matrix interfacial microcracking. Another aspect to be considered in this context is the fact that lead has negligibly small solid solubility with copper and/or tin,<sup>[24]</sup> with the result that the element exists in the bronze as discrete particles (Figure 1(a), regions marked by C) having poor (although metallurgical) lead/matrix interfacial bonding.<sup>[8]</sup> The poor lead/matrix interfacial bonding facilitates the initiation followed by the propagation of microcracks along the interfacial regions in the bronze. This is especially so at lower operating temperatures, like at 0.42 m/s (Figure 5(a)), wherein the  $\alpha$  phase possesses poor compatibility.<sup>[8]</sup> Similar observations have also been made in aluminum alloy-particle composites.<sup>[25]</sup> Under the circumstances, the soft and weak lead particles act as porosity/weak points and favor poor mechanical properties (Table II and Figure 3) and inferior wear characteristics (Figure 4), the latter caused by material chipping off, leading to premature removal of the microconstituents in the form of very coarse debris particles.<sup>[8,9]</sup> On the contrary, however, when the degree of frictional heating is sufficiently high, like the one at 4.60 m/s (Figure 5(b)), the  $\alpha$  phase attains improved compatibility, provides a better support to the remaining microconstituents, and enables the latter ones to produce their positive effects<sup>[8,26]</sup> more efficiently in view of the reduced tendency of the alloy toward

microcracking.<sup>[8,9]</sup> As a result, the wear rate of the leaded-tin bronze was reduced considerably at 4.60 m/s over the one at 0.42 m/s (Figure 4).

In the case of the aluminum bronze, there does not exist any effective lubricating phase, but the alloy attains excellent hardness and compressive strength at room temperature, as shown in Table II. It also exhibits good tensile properties even at elevated temperatures (Figure 3) because of the presence of the fine particles of ( $\delta$ ) iron<sup>[4,27]</sup> and Cu-Al precipitates along with  $\alpha$  (copper-rich solid solution of aluminum), as shown in Figure 1(b), regions marked A, D, and arrow, respectively. As a result, the question of microcracking practically does not arise in the absence of a crack-sensitive phase (e.g., lead in the leaded-tin bronze). This led to better wear response of the alloy over the leaded-tin bronze at the lower sliding speed (Figure 4). However, the absence of an effective lubricating phase in spite of excellent elevated temperature properties (Figure 3) adversely affected the wear characteristics of the aluminum bronze over that of the latter (Figure 4).

Specific microstructural features of the zinc-based alloy include the presence of basically a mixture of two soft and ductile zinc- and aluminum-rich solid solutions ( $\alpha$  and  $\eta$ , respectively) distributed in a specific manner along with a minor quantity of  $\epsilon$  (Figure 1(c), regions marked by A, E, and double arrow, respectively). The major microconstituent ( $\eta$ ) is lubricating in nature and carries load along with  $\alpha$ .<sup>[10]</sup> The alloy also possessed far improved mechanical properties over the leaded-tin bronze at room temperature (Table II and Figure 3). However, the strength of the zinc-based alloy deteriorated drastically at higher test temperatures, unlike the bronzes (Figure 3), due to low melting characteristics of the former. This caused the zinc-based alloy to perform better during the wear tests at 0.42 m/s (Figure 4) due to less frictional heating (Figures 5(a) and 6); in fact, the alloy showed minimum wear loss (prior to seizure) amongst all these materials (Figure 4). On the contrary, a larger sliding speed (i.e., 4.60 m/s) caused the generation of a higher rate of frictional heating (Figures 5(b) and 6), leading to the most inferior wear response of the zinc-based alloy (Figure 4). Thus, in spite of good lubricating properties, poor elevated strength of the zinc-based alloy (Figure 3) led to deterioration in its wear behavior at the higher sliding speed (Figure 4).

A comparison of the wear response of the alloys clearly indicates the best wear performance of the zinc-based alloy at 0.42 m/s (Figure 4) to be due to less frictional heating (Figures 5(a) and 6), the latter enabling its microconstituents to play their roles effectively. In this case, the predominance of the crack-sensitive nature of the lubricating-phase lead caused material chipping off as a result of less generation of frictional heat (Figures 5(a) and 6), ultimately leading to the most inferior wear performance for the leaded-tin bronze (Figure 4). The aluminum bronze attained an intermediate wear response (Figure 4) in spite of the absence of a lubricating phase. This could be attributed to the absence of a crack-sensitive phase, unlike the case of the leaded-tin bronze. On the contrary, at 4.60 m/s of sliding speed, the trend changed entirely in the sense that a sufficient degree of frictional heat generated during wear tests (Figures 5(b) and 6) suppressed the microcracking tendency of the leaded-tin bronze arising out of the presence

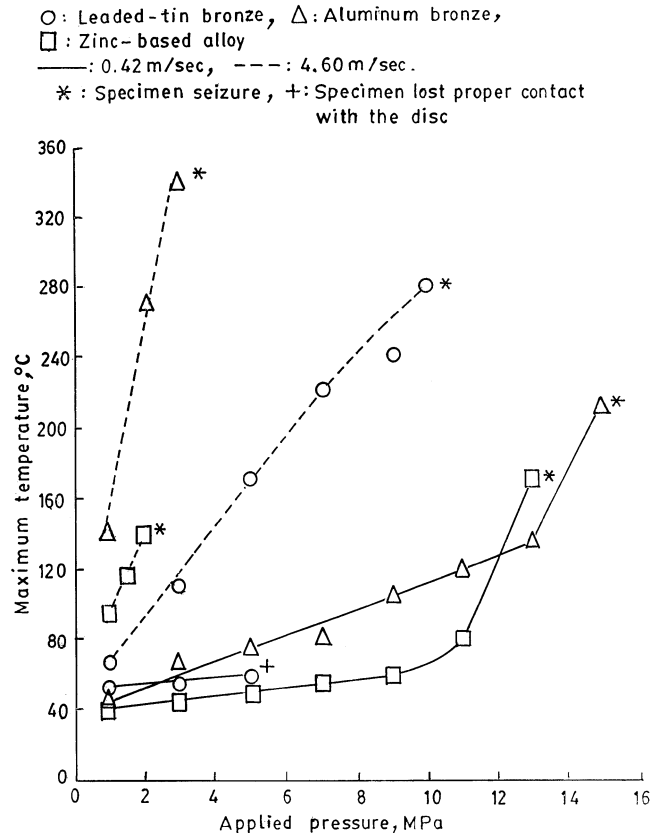


Fig. 6—Maximum temperature rise (near the specimen surface) vs pressure plots at different sliding speeds.

of lead, thereby forming a lubricating film of lead on the specimen surface.<sup>[8,26]</sup> This, in turn, caused the leaded-tin bronze to exhibit the best wear resistance among all the alloys (Figure 4). In spite of a very high thermal stability (Figure 3), the aluminum bronze performed far inferior to that of the leaded-tin bronze at 4.60 m/s (Figure 4) because no lubricating phase was present in the former case. However, very good thermal stability (in the absence of a lubricating phase) of the aluminum bronze (Figure 3) could only help to improve its wear performance slightly over that of the zinc-based alloy (Figure 4), although the latter had much inferior elevated temperature properties (Figure 3) but good lubricating characteristics.<sup>[10]</sup> Interestingly, the leaded-tin bronze performed far better than that of the zinc-based alloy (Figure 4), although the former attained much less room temperature hardness (Table II).

A critical appraisal of the observations made so far clearly suggests that the dry sliding wear response of a material greatly depends on the predominance of the nature of its lubricating and load-bearing constituents, thermal stability, and crack sensitivity. Room temperature properties, such as compressive and tensile strengths and hardness, do not give a meaningful indication as far as the wear resistance of the materials involving high operating temperatures is concerned. However, room temperature properties could serve some purpose with regard to low sliding speed tests wherein limited frictional heat is generated. Interestingly, in some cases like the leaded-tin bronze, this higher degree of heating produced favorable results, while in other varieties of the alloys, such as the aluminum bronze and

the zinc-based, it proved detrimental. Accordingly, elevated temperature properties could give better indications concerning the wear resistance of materials. Thus, it becomes apparent that a material should have a good balance of thermal stability and lubricating characteristics in order to derive better dry sliding wear properties. The microcracking tendency of the material, for whatever reason, is definitely detrimental in this regard and hence should be avoided as much as possible.

## V. CONCLUSIONS

1. The leaded-tin bronze performed poorly at the lower sliding speed (*i.e.*, at 0.42 m/s) due to the predominance of the cracking tendency of the lubricating lead particles under the conditions of less frictional heating. The zinc-based alloy exhibited its wear resistance to be much superior to that of the leaded-tin bronze because of good lubricating characteristics of the former. The aluminum bronze, in spite of not containing any lubricating phase, attained better seizure resistance than the zinc-based alloy. The absence of a crack-sensitive phase showed better wear characteristics of the zinc-based alloy and the aluminum bronze over the leaded-tin bronze at low speed.
2. At the sliding speed of 4.60 m/s, generation of a sufficiently high degree of frictional heat suppressed the microcracking tendency of the leaded-tin bronze, leading to the formation of lubricating lead film on the specimen surface. This ultimately caused much better wear performance of the leaded-tin bronze over the one at lower speed. Further, the leaded-tin bronze also showed its wear characteristics to be much superior to those of the zinc-based alloy and the aluminum bronze, despite having less thermal stability than the aluminum bronze and much less lubricating phase than that of the zinc-based alloy. Interestingly, the leaded-tin bronze also possessed much less hardness and tensile strength at room temperature than the remaining alloys. Better thermal stability of the aluminum bronze could help it to attain somewhat better wear resistance than the zinc-based alloy because of the absence of a lubricating phase in the former case.
3. It is essential for a material to attain a good balance of thermal stability and lubricating characteristics in order for it to show improved wear performance. A microcracking tendency of the material produces a detrimental effect, at least at low operating temperatures, and hence is undesirable. Attempts therefore should be made to avoid such a situation. In fact, the predominance of the mentioned factors greatly controls the wear response of materials, which in turn is governed by the conditions of sliding.

4. Room temperature mechanical properties, such as hardness and tensile and compressive strengths, could give an indication of the wear resistance of materials under low operating temperature conditions, be it due to low speed of sliding or pressure. However, they fail to bear any correlation with severe wear conditions leading to the generation of high frictional heat. Accordingly, elevated temperature mechanical properties become meaningful to predict the wear response of materials under high operating temperature conditions of wear, and room temperature mechanical properties play rather a secondary role in this context.

## REFERENCES

1. G.C. Pratt: *Int. Met. Rev.*, 1973, vol. 18, pp. 1-27.
2. E.J. Kubel, Jr.: *Adv. Mater. Processes*, 1987, vol. 132, pp. 51-57.
3. *Metals Handbook*, 1st ed., ASM, Metals Park, OH, 1992, vol. 18, pp. 515-22.
4. *Copper and Its Alloys*, E.G. West, ed., Ellis Horwood Publishers, Chichester, Sussex, England, 1982, pp. 84-131.
5. A.K. Woolaston: *Copper Alloy Bearing Materials*, Technical Note (TN9), Copper Development Association, London.
6. T.S. Calayag: *Mining Eng.*, 1983, vol. 35, pp. 727-28.
7. D. Rollez, M. Meeus, and L. Groothaert: *Proc. Int. Symp. Zinc-Aluminium (ZA) Casting Alloys*, Toronto, Aug. 17-20, 1986, G.P. Lewis, R.J. Barnhurst, and C.A. Loong, eds., CIM, Montreal, 1986, pp. 315-22.
8. B.K. Prasad, A.K. Patwardhan, and A.H. Yegneswaran: *Mater. Sci. Technol.*, 1996, vol. 12, pp. 427-35.
9. W.A. Glaeser: *Proc. Int. Conf. Wear Materials*, Apr. 9-13, 1989, Denver, CO, K.C. Ludema, ed., ASME, Fairfield, NJ, 1989, vol. I, pp. 255-60.
10. S. Murphy and T. Savaskan: *Wear*, 1984, vol. 98, pp. 151-61.
11. B.K. Prasad: Ph.D. Thesis, University of Roorkee, Roorkee, IN, 1994.
12. B.K. Prasad: *Z. Metallkd.*, 1996, vol. 87, pp. 226-32.
13. T. Savaskan and S. Murphy: *Wear*, 1987, vol. 116, pp. 211-24.
14. J.P. Pathak: *Mater. Sci. Technol.*, 1993, vol. 9, pp. 403-07.
15. P.P. Lee, T. Savaskan, and E. Laufer: *Wear*, 1987, vol. 117, pp. 79-89.
16. T. Ma, Q.D. Chen, S.C. Li, and H.M. Wang: *Proc. Int. Conf. Wear Materials*, Apr. 9-13, 1989, Denver, CO, ASME, Fairfield, NJ, 1989, vol. I, pp. 297-304.
17. J.P. Pathak and S.N. Tiwari: *Wear*, 1992, vol. 155, pp. 37-47.
18. V.E. Buchanan, P.A. Molian, T. Sudarshan, and A. Akers: *Wear*, 1991, vol. 146, pp. 241-56.
19. P.A. Molian, V.E. Buchanan, T.S. Sudarshan, and A. Akers: *Wear*, 1991, vol. 146, pp. 257-67.
20. P.J. Blau: *Wear*, 1984, vol. 94, pp. 1-12.
21. J.J. Wert, S.A. Singerman, S.G. Caldwell, and D.K. Chaudhuri: *Wear*, 1983, vol. 92, pp. 213-29.
22. J.J. Wert and W.M. Cook: *Wear*, 1988, vol. 123, pp. 171-92.
23. F.E. Kennedy, Jr.: *Wear*, 1984, vol. 100, pp. 453-56.
24. *Friction and Wear of Materials*, E. Rabinowicz, ed., John Wiley & Sons Inc., New York, NY, 1965, pp. 84-131.
25. B.S. Mazumdar, A.H. Yegneswaran, and P.K. Rohatgi: *Mater. Sci. Eng.*, 1984, vol. 68, pp. 85-96.
26. S. Das and B.K. Prasad: *Wear*, 1993, vols. 162-164, pp. 64-74.
27. *Foundry Metallography: An Elementary Analysis of Microstructure and Properties of Selected Foundry Alloys*, A.R. Bailey and L.E. Samuels, eds., Metallurgical Services, Betchworth, Surrey, England, 1976.